Characteristics of lightning flashes with exceptional illuminated areas, durations, and optical powers and surrounding storm properties in the tropics and inner subtropics

Michael Peterson[1] and Chuntao Liu[2]

Received 4 April 2013; revised 3 August 2013; accepted 7 August 2013; published 24 October 2013.

[1] Twelve years (1998–2009) of Lightning Imaging Sensor (LIS) observations are used to characterize lightning flashes by illuminated area, duration, and optical power, particularly for exceptional flashes defined as those above the 90th percentile of each parameter. Statistics of lightning are summarized over land, ocean, and coastal regions of the Tropical Rainfall Measuring Mission satellite's domain extending from 36°S to 36°N. The degree to which optical flash parameters are interrelated is discussed, as well as coincident environmental properties and the overall characteristics of parent thunderstorms. LIS flashes over the southern United States are also collocated to National Lightning Detection Network (NLDN) observations, and relationships between LIS optical flash properties and corresponding NLDN strengths are discussed. Daytime (nighttime) oceanic flashes are shown to be 31.7% (39.4%) larger and 55.2% (75.1%) brighter in terms of maximum event pixel radiance. At the same time, daytime (nighttime) coastal flashes have 22.1% (7.8%) longer durations than flashes over land and 15.6% (11.4%) longer durations than oceanic flashes. Particularly, large and bright flashes observed by LIS are typically centered in weak storm regions, but thunderstorms with exceptional flashes are, themselves, more intense overall than those with only small and dim flashes. Diurnally, the top 10% brightest lightning flashes peak about 2 h earlier than the top 10% largest and long-lasting flashes over land, implying that lightning flash characteristics vary with the life cycle of thunderstorms. Larger and more radiant flashes are also shown to be associated with stronger NLDN flashes of positive and negative polarity.

Citation: Peterson, M., and C. Liu (2013), Characteristics of lightning flashes with exceptional illuminated areas, durations, and optical powers and surrounding storm properties in the tropics and inner subtropics, *J. Geophys. Res. Atmos.*, *118*, 11,727–11,740, doi:10.1002/jgrd.50715.

1. Introduction

[2] Lightning flashes come in all shapes and sizes, ranging from direct cloud-to-ground discharges to expansive intracloud flashes, and have even been observed in some cases to extend dozens of kilometers between convective cores [*Kuhlman et al.*, 2009; *Betz et al.*, 2009]. Expansive lightning discharges are rather rare and often involve different parts of the parent storm, including the stratiform region. Regions of charged stratiform precipitation behind the leading line of a storm consist of stacked horizontal layers of alternating polarity that are thought to serve as conduits for lightning propagation [*Marshall and Rust*, 1993; *Stolzenburg et al.*, 1994; *Lang et al.*, 2004; *Carey et al.*, 2005; *Marshall et al.*, 2009]. There are also studies showing that high amplitude lightning discharges detected by very low frequency electromagnetic sensors occur more often over the ocean than over land [*Füllekrug et al.*, 2002], and that lightning flashes appear to be larger and brighter over the ocean as seen from optical sensors in space [*Turman*, 1977; *Boccippio et al.*, 2002]. However, given the limited samples used in these studies, regional differences could not be described quantitatively in detail on a global scale.

[3] The goal of this study is to use long-term observations from the Tropical Rainfall Measuring Mission (TRMM) satellite to provide a global scale climatology of exceptionally large, bright, and long-lasting lightning flashes and their properties. The TRMM satellite [*Kummerow et al.*, 1998] is a low-earth orbiting satellite with a domain that includes the global tropics and parts of the subtropics. Its sensor package includes a Lightning Imaging Sensor (LIS), a precipitation radar (PR), a microwave imager (TMI), and a visible and infrared scanner (VIRS). TRMM was launched in December of 1997 and has been in orbit for more than 15 years at the time of writing, providing a robust data set of storm observations from its various sensors.

[1]Department of Atmospheric Sciences, University of Utah, Salt Lake City, Utah, USA.
[2]Department of Physical and Environmental Sciences, Texas A&M University at Corpus Christi, Corpus Christi, Texas, USA.

Corresponding author: M. Peterson, Department of Atmospheric Sciences, University of Utah, 135 S. 1460 E., Rm 819, Salt Lake City, UT 84112, USA. (michael.j.peterson@utah.edu)

2169-897X/13/10.1002/jgrd.50715

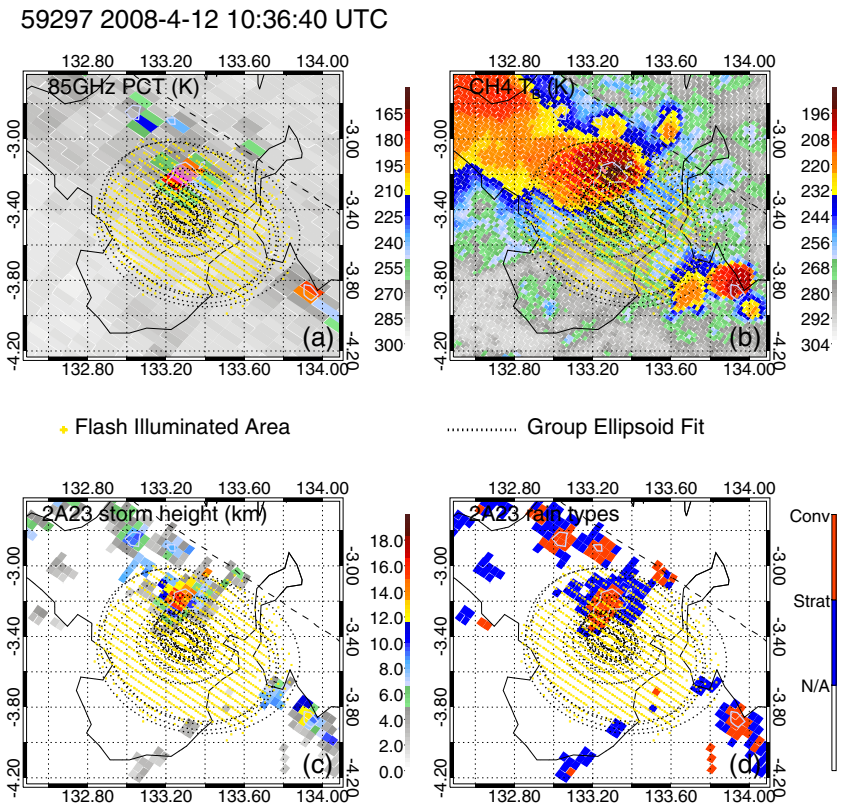

Figure 1. An example of a LIS-observed lightning flash that illuminates a large area. The centers of illuminated pixels are indicated by yellow crosses, while dotted lines outline ellipsoid fits of groups of event pixels at a particular time. (a)TMI 85 GHz PCTs, (b) VIRS CH4 IR brightness temperatures, (c) 2A23 storm heights (~18 dBZ echo top height) and (d) 2A23 rain types [*Awaka et al.*, 1998] are shown.

[4] The Lightning Imaging Sensor (LIS) is an optical transient detector that observes lightning by looking for departures from background radiance in the near infrared at 777 nm that are characteristic of lightning flashes. Event pixels that are determined to be the result of lightning are grouped in space and time into individual lightning flashes by the LIS algorithms [*Christian et al.*, 2003; *Mach et al.*, 2007]. There have been a number of studies combining LIS, PR, and TMI observations in order to examine relationships between the properties of thunderstorms and the frequency of lightning flashes [e.g., *Boccippio et al.*, 2000; *Toracinta et al.*, 2002; *Cecil et al.*, 2005; *Peterson and Liu*, 2011; *Liu et al.*, 2011; *Liu et al.*, 2012]. However, there is still a lack of research examining the LIS optical properties of lightning flashes.

[5] In this study, lightning flashes observed by LIS are categorized by their illuminated area, duration, total, peak and mean radiance, and mean optical power. Due to significant land-ocean differences in lightning properties and electric fields that have been observed in previous studies [*Boccippio et al.*, 2000; *Mach et al.*, 2010; *Mach et al.*, 2011], LIS flashes are categorized by terrain type (land, ocean, or coast) and differences in LIS optical properties between each group are explored. There are a number of caveats with LIS data that may have some effect, such as the diurnal variation of the LIS instrument sensitivity and cloud attenuation of lightning flash radiance. For this reason, PR and TMI observations coincident with flash center locations are analyzed and the potential effects of these environmental properties on flash characteristics are also discussed.

2. Data and Methodology

[6] Twelve years of TRMM observations from 1998 through 2009 are considered in this study, which include more than 6 million lightning flashes within the Precipitation Radar (PR) field-of-view. The LIS sensor identifies illumination from lightning flashes at three scales: event pixels, groups, and flashes [*Mach et al.*, 2007]. Figure 1 shows an example of TRMM observations of 85 GHz Polarization Corrected Temperature (PCT) [*Spencer et al.*, 1989], VIRS infrared brightness temperature, storm height from the 2A23 algorithm [*Awaka et al.*, 1998, 2009], and precipitation type, also determined by 2A23. The features that make up the lightning flash shown—one of the largest flashes observed by LIS—are overlain in each panel.

[7] The smallest, most basic features, elements of the flash in Figure 1 are event pixels. They are defined as individual LIS pixels that are consistent with optical transients from lightning. Event pixels are shown as yellow plus signs in the figure. Event pixels, or just events, are significantly more radiant than the constantly changing background radiance

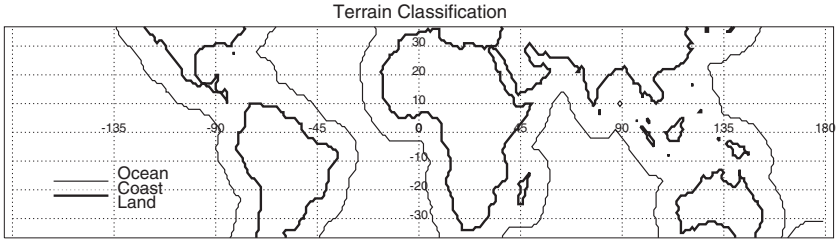

Figure 2. Global terrain type classification. Open ocean regions are separated from coastal areas by thin lines, and coastal regions (within 1000 km of major continents) are separated from land by thick lines.

and are detected throughout the ~80 s observation window of the LIS sensor.

[8] Contiguous events observed at the same instance are then combined into the next scale of LIS feature: the LIS group. Groups summarize the properties of the illuminated region of events at a particular time. Group parameters include group area, total radiance—calculated as the sum of all of its child events—and minimum, mean, and maximum event radiance. Ellipsoid fits for each of the groups that comprise the flash in Figure 1 are shown in the figure. Even though they correspond to the same flash, many of these groups are vastly different from the others with drastically different sizes and eccentricities.

[9] Finally, LIS groups are combined into individual lightning flashes by the LIS algorithms. Group-to-flash associations are carried out using a weighted Euclidian distance method with distance thresholds of 5.5 km and a time threshold of 330 ms [*Mach et al*., 2007]. Flashes integrate the properties of events and groups. Since flashes are not confined to a single observation time, their durations can also be determined by examining the length of time between the first and last observed group. If a particular flash is only composed of one group, however, its duration would be determined to be 0 s, which is not physical. Since the LIS integrates radiance over 2 ms intervals [*Mach et al*., 2007], single-group flashes may occur at shorter time scales, may not be fully detected by the LIS, or may be artifacts. The additional time component of flashes also makes their illuminated areas distinct from groups. Unlike groups, whose areas are defined as the sum of the areas of each of their component events, flashes typically include overlapping groups and events. Instead of just taking the total of the component event areas, flash illuminated area is defined as the overall footprint area of the flash events (the total yellow area in Figure 1). Flash mean optical power is then calculated for flashes with finite recorded durations by dividing their mean event radiances by their durations. For additional details about the LIS clustering algorithms, please refer to *Mach et al*. [2007].

[10] One of the major concerns with using an optical sensor like LIS to observe lightning is the possibility of attenuation and scattering by the surrounding cloud. Two similar flashes —one occurring in a storm region with a relatively high total ice water depth, and one occurring in a storm region with little to no ice—could appear very different when viewed by the LIS. Fortunately, the TRMM satellite has additional instruments that can reveal information about nearby storm structure. TRMM PR and TMI observations are combined with LIS flashes using two different methods. First, the geometric centers of lightning flashes are used to colocate LIS flashes to individual pixel-level observations from the other sensors using the same methodology employed by *Peterson and Liu* [2011]. These data provide information about radar reflectivity and microwave scattering in the center of the viewing environment. Flash centers are also used to categorize flashes by terrain type as inland, coastal, or open ocean, following the mask shown in Figure 2. The second method used to tie LIS flashes to other TRMM observations is by assigning flashes to nearby PR-observed raining areas (Radar Precipitation Features (RPFs)) [*Liu et al*., 2008]. This method allows for optical flash characteristics to be examined in the context of overall storm properties. The method used to associate lightning flashes to radar features is different from that used in *Peterson and Liu* [2011]. Instead of employing the nearest neighbor method, flash center locations are compared directly to RPF index masks, making it less ambiguous which feature a flash that corresponds to in the event of multiple nearby features. This, however, also introduces a new constraint on the sample, requiring that flashes must not only fall within the PR swath but that they also must occur within raining storm regions. The result of this restriction is a reduction of the sample size by nearly a half a million flashes, leaving an overall sample size of 5.5 million flashes.

[11] Diurnal variations of the sensitivity of the LIS are also a concern since the classification of an event pixel corresponding to lightning activity depends on the difference of its radiance from the observed background radiance, which varies significantly diurnally. It has been noted [*Mach et al*., 2007] that during the day, the dimmest flashes often go undetected due to the increased brightness of the background radiance. For the same reason, dim event pixels around the periphery of groups belonging to any flash may also not be easily distinguished from the background during the day, resulting in a potentially smaller optical footprint. For this reason, it would appear necessary to break up the day into periods of similar LIS sensitivity in order to prevent sensitivity bias from influencing the statistics of optical properties. Median, 90th percentile and 99th percentile values of the lowest minimum event radiance observed in flashes over land, ocean and, coastal regions are shown in Figure 3a. The minimum detected event radiances are lower at night when the sensitivity is relatively high and the sensor is able to detect dimmer events, and higher during the day when those dim pixels would go undetected. There are also two transition periods in the morning (T1) and evening (T3) due to the sunrise, sunset, and varying day length with the changing seasons. However, during the daytime and at nighttime periods, there is little variation in these statistics, even for the lowest percentile curves. This leads to a natural division of the diurnal sensitivity cycle into

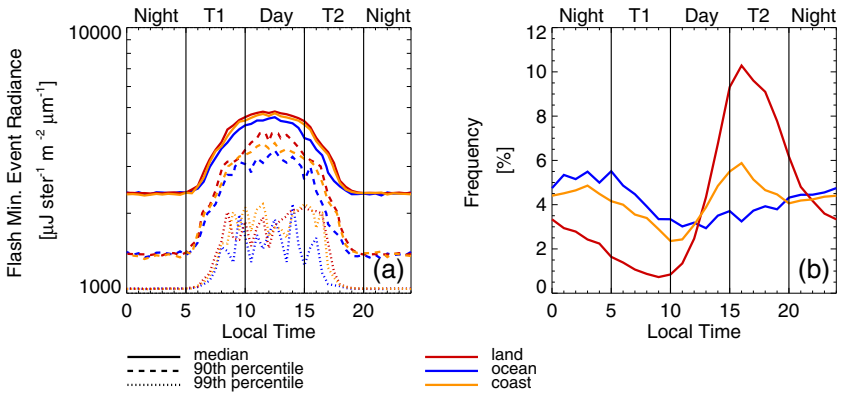

Figure 3. Diurnal variation of LIS sensitivity demonstrated by the median, 90th, and 99th percentile of (a) flash minimum event radiances and (b) diurnal sample density for flashes corresponding to each terrain type.

two different regimes of relatively constant sensitivity: a daytime sensitivity regime (10:00–15:00 LT) and a nighttime sensitivity regime (20:00–05:00 LT). Due to substantial differences in the diurnal cycles of lightning flashes over land and over the ocean (Figure 3b) following diurnal patterns of convection [*Hendon and Woodberry*, 1993; *Nesbitt and Zipser*, 2003; *Liu and Zipser*, 2008; *Lay et al*., 2007], it would be problematic to directly compare the properties of all oceanic flashes (which mostly occur at night) to those over land (which mostly occur during the day). Therefore, the properties of lightning flashes that occur over each of the three terrain types shown in Figure 2 are examined separately for the daytime and nighttime sensitivity regimes of Figure 3, leading to six categories of flashes determined by terrain type and instrument sensitivity.

[12] Such a division of the day by LIS sensitivity is not without drawbacks, however. An important caveat this partitioning introduces is a major reduction in the sample size, which affects land, oceanic, and coastal flash categories differently. The peak frequency of oceanic flashes occurs well within the nighttime sensitivity regime shown in Figure 3b, but a large portion of flashes over land, including

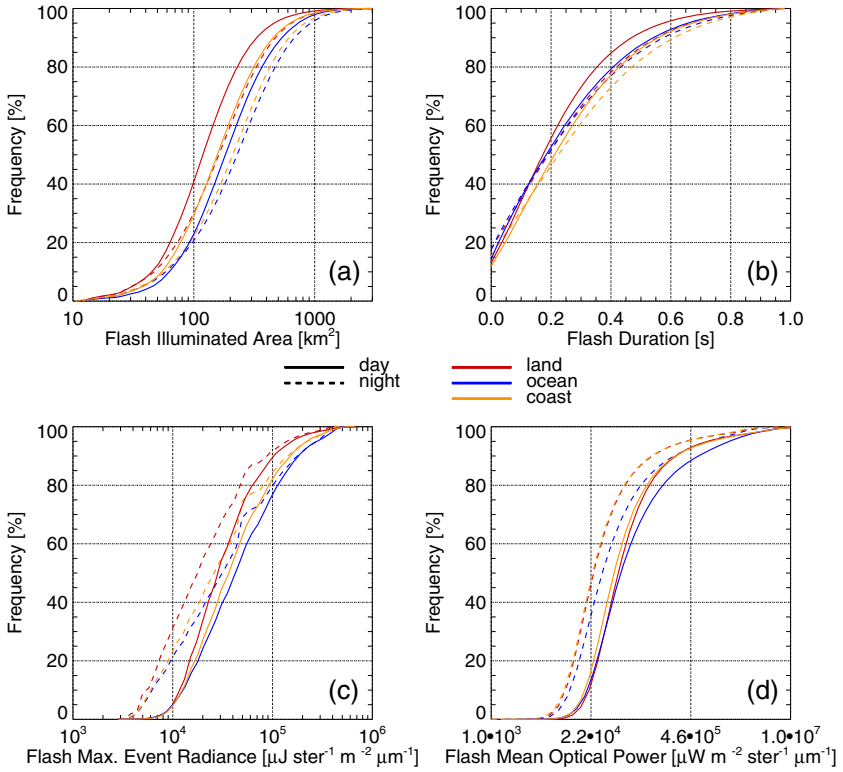

Figure 4. Cumulative Distribution Functions (CDFs) of (a) flash illuminated area, (b) flash duration, (c) flash maximum event radiance, and (d) flash mean optical power of LIS flashes categorized by terrain type and LIS sensitivity regime.

Table 1. Median and 90th Percentile Threshold Values for Flash Illuminated Area, Duration, and Mean Optical Power for Flashes in Each Sensitivity Regime and Terrain Category

		Day		Night	
	Terrain	Median	Top 10%	Median	Top 10%
Flash area (km^2)	all	148.6	604.8	206.4	839.7
	land	137.4	533.8	189.1	751.9
	ocean	211.5	840.4	267.6	1,085.3
	coast	181.2	724.8	246.7	980.8
Flash duration (s)	all	0.20	0.65	0.22	0.75
	land	0.19	0.61	0.21	0.73
	ocean	0.21	0.72	0.21	0.78
	coast	0.24	0.74	0.25	0.82
Flash mean optical Power ($\mu W\ m^{-2}\ ster^{-1}\ \mu m^{-1}$)	all	62,512	1,083,060	31,440	565,709
	land	63,893	1,000,030	30,982	523,655
	ocean	68,969	1,956,580	40,111	1,075,970
	coast	57,446	1,127,510	31,132	559,729

the peak of the diurnal distribution, actually occurs just outside of the daytime sensitivity regime in the time period defined as the T2 transition zone. These diurnal cycles are consistent with past literature [e.g., *Mach et al*., 2011; *Blakeslee et al*., 2012], but their timing relative to LIS sensitivity leads to a higher probability of oceanic flashes being included in their respective categories than flashes over land. However, even though this restriction reduces the overall sample by nearly half, given the enormity of the original sample and the relative abundance of flashes over land, the effect of this preferential selection of oceanic flashes on the overall statistics would be marginal, at best.

3. Results

3.1. Optical Properties of LIS Lightning Flashes

[13] Cumulative distribution functions (CDFs) of flash illuminated area, duration, maximum event radiance, and mean optical power are shown in Figure 4 for land, ocean, and coastal flashes. Differences in flash properties between the daytime and nighttime sensitivity regimes are easily observed in these statistics. Daytime flashes tend to have smaller optical footprints (Figure 4a), higher mean optical powers (Figure 4d), and brighter maximum event radiances (Figure 4c) than nighttime flashes for all three terrain types, which is to be expected since the increased sensitivity at night would allow dimmer areas of flashes to be seen, while daytime flash observations would be biased toward flashes with more radiant event pixels.

[14] Differences between flashes over the various terrain types within the same sensitivity regime are also evident. As shown in Table 1, the mean illuminated area of oceanic flashes is 31.7% greater during the day and 39.8% greater at night compared to flashes over land, with coastal flashes falling in between the other two terrain types. Oceanic flashes also tend to be more radiant than flashes over land, not only with regards to mean optical power, which is 24.6% higher over the ocean during the day and 41.2% brighter over the ocean at night, (Figure 4c), but with maximum event radiance as well, which is 55.2% greater over the ocean during the day and 75.1% greater at night (Figure 4d). Flash durations (Figure 4b) are similar between flashes over land and the open ocean for both sensitivity regimes. However, coastal flashes tend to have slightly longer durations compared to land and ocean flashes, setting themselves apart from the other terrain classifications. Coastal flashes have 22.1% (7.8%) longer durations than land (ocean) flashes during the day and 15.6% (11.4%) longer durations at night (Figure 4b). Though not as large of a difference as the land-ocean contrasts observed for radiance and illuminated area, given the large sample size, this trend is still statistically significant. Despite changes in sensitivity throughout the day, each of these trends is evident in each sensitivity regime with the primary differences lying in the magnitudes of the contrasts and the values of the distribution. Even though the diurnal sensitivity variation of the LIS has a significant effect on the perceived optical properties of the observed lightning flashes, most of the trends addressed in this study (such as those in Figure 4) can be observed in each sensitivity regime. For this reason, unless there are significant differences between nighttime and daytime trends, only nighttime analyses are shown from this point further.

[15] The land-ocean differences shown in Figure 4 are by no means homogeneous across the globe. In order to examine regional trends, regional thresholds of large, long-lasting, and bright nighttime flashes are shown in Figure 5. In this figure and elsewhere, exceptional flashes are defined by the 90th percentile of the parameter of interest, in this case, illuminated area, duration, and mean optical power, respectively. While much of the open ocean lacks sufficient samples to be statistically relevant, it is evident in Figure 5a that oceanic regions, in general, have higher thresholds for the 90th percentile of flash illuminated area than land regions. Sharp gradients in flash area can be observed along coastlines such as the western coast of Mexico and the coast of Vietnam. This is consistent with Figure 4, where coastal CDFs fall in between those for land and ocean. However, some coastal regions have flash sizes similar to those found over nearby oceanic regions. The maritime continent [*Williams*, 2005], for example, does not deviate from the statistics from the surrounding waters of the western Pacific. At the same time, the Amazon, known as the "green ocean" [*Williams and Sátori*, 2004] has flash size statistics that are more consistent with a continental rather than an oceanic climate.

[16] Particularly, bright flashes—those that fall above the 90th percentile of flash mean optical power shown in Table 1—are also fractionally more common over the ocean than over land, similar to large flashes, thus leading to higher regional 90th percentile values of optical mean power in Figure 5b. However, regions associated with the highest

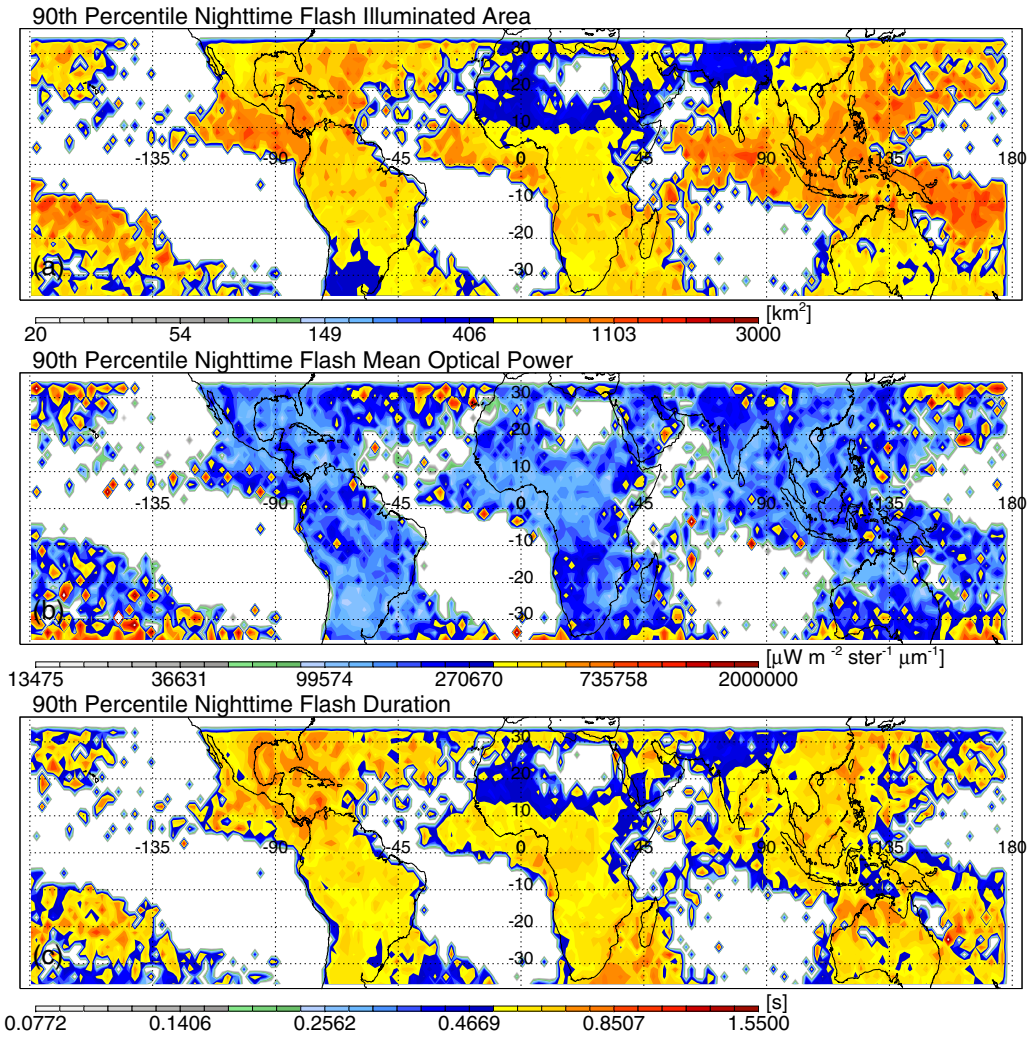

Figure 5. Regional distributions of nighttime 90th percentile thresholds for (a) flash illuminated area, (b) flash mean optical power, and (c) flash duration for 2° by 2° boxes within the TRMM domain. Results are only shown for boxes with more than 20 samples.

thresholds of mean optical power are different than those most associated with large flashes. While 90th percentile values in excess of 750 km^2 in Figure 5a tend to be concentrated within 20° of the equator, regions with the brightest flashes are mostly located poleward of 25° latitude. At the same time, regions with high thresholds for 90th percentile flash duration (Figure 5c) can be found at all latitudes within the TRMM domain. They are at times coincident with regions of large flashes and bright flashes, and are often found in coastal regions rather than throughout the open ocean, as the flash duration statistics in Figure 4b suggest.

[17] Of course, high fractional occurrence does not always indicate a large abundance of flashes. Figure 6 shows global distributions of nighttime large (Figure 6a), long-lasting (Figure 6b), and bright (Figure 6c) flashes overall, based on the 90th percentile global thresholds listed in Table 1. Regions that tend toward large flashes, such as the western Central American coast, the South Pacific, and the equatorial Indian Ocean, only account for a small portion of large flashes globally, while high numbers of exceptionally large flashes can be found in continental regions such as the Congo basin, Argentina, and the Southern United States. The same can be said for long-lasting lightning flashes (Figure 6b) and optically bright lightning flashes (Figure 6c). By sheer numbers, exceptional lightning flashes occur in these regions more than any other due to the fact that they see more lightning than anywhere else, but as a fraction of total lightning, these exceptional flashes are somewhat rare compared to the regions that stand out in Figure 5.

3.2. Relationships Among Flash Size, Duration, and Optical Power

[18] Since the LIS detects lightning from the optical signature it leaves, the same factors that influence LIS-observed optical radiance may also have an effect on LIS observations of illuminated area and duration. Even though regions with larger, brighter, and longer-lasting flashes are not always coincident in Figure 6, it is still possible that flash illuminated area, brightness, and duration may, in fact, be related to one another in some way. All three parameters depend on how a lightning flash illuminates its surrounding cloud region and how this illumination is seen by the LIS. Linear correlation coefficients between LIS flash illuminated area, duration, mean event radiance, maximum event radiance, and

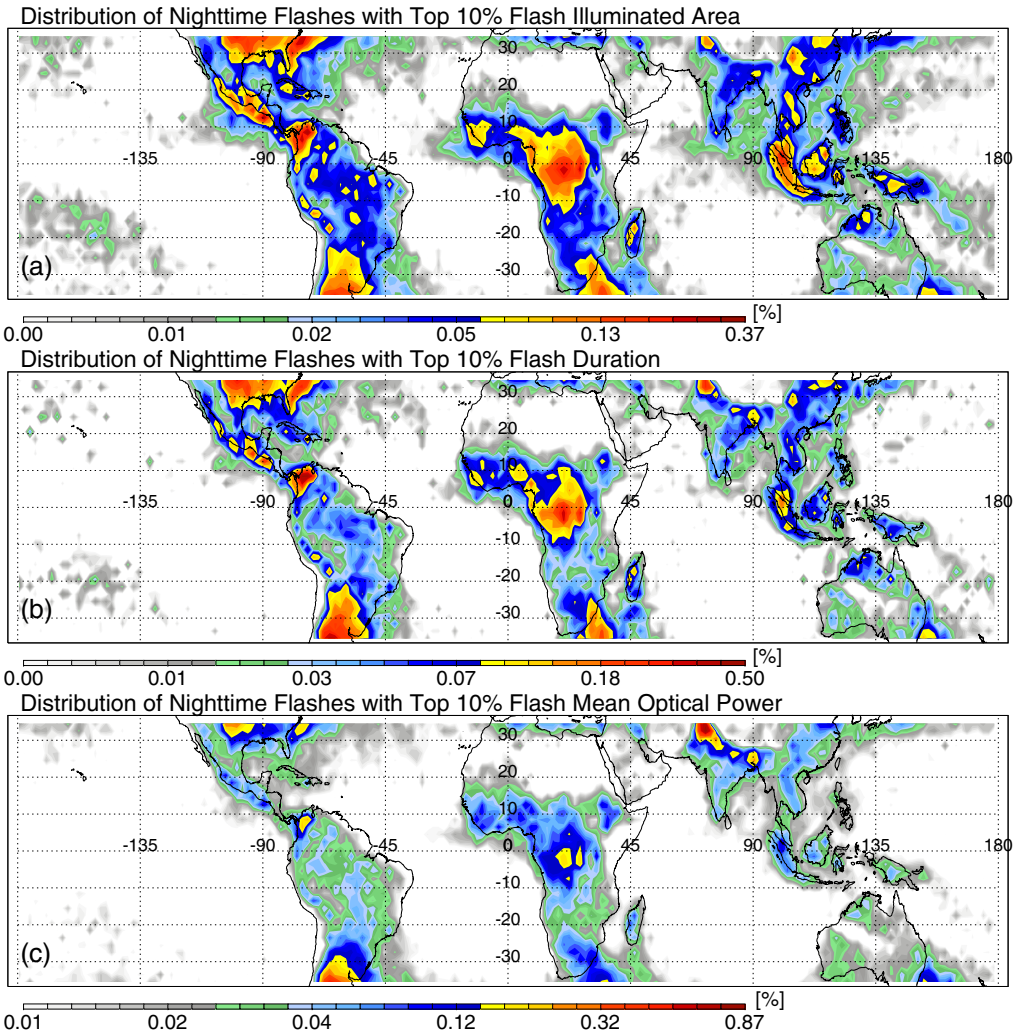

Figure 6. Global distribution of nighttime flashes with (a) exceptional (top 10%) illuminated area (>604 km^2), (b) duration (>0.65 s), and (c) mean optical power ($>1.08 \times 10^6$ $\mu W\ m^{-2}\ ster^{-1}\ \mu m^{-1}$).

mean optical power are given in Table 2 for all flashes. None of these correlation coefficients are outstanding, with flash duration nearly as well correlated with flash area and maximum event radiance with correlation coefficients of 0.39 and 0.38, respectively, and flash area and maximum event radiance more highly correlated with a correlation coefficient of 0.56. At the same time, mean optical power, which is a measure of the overall brightness of a flash, shows hardly any correlation with any of the other parameters (ranging from 0.01 to 0.16), even though it is calculated from flash mean event brightness and duration.

[19] These weak correlations are also demonstrated in Figure 7 with two-dimensional histograms of flash area and either flash duration (a and b) or maximum event radiance (c and d) for both daytime and nighttime flashes. For both oceanic and land-based flashes in each sensitivity regime, flashes with smaller illuminated areas tend to have shorter durations, and large flashes are more likely to have very long durations, but there is hardly a direct correspondence between these two parameters. Changing from a linear to a logarithm model improves the correlation between flash illuminated area and flash duration from 0.39 to 0.51, which is still quite low.

[20] With a peak correlation coefficient of just 0.56 between flash maximum radiance and flash area, it is clear that these factors, alone, do not explain the observed variance in flash illuminated area. It may be that particularly radiant flashes could illuminate large areas of clouds by scattering alone, regardless

Table 2. Linear Correlation Coefficients Between LIS Optical Flash Properties

	Duration	Mean Event Radiance	Maximum Event Radiance	Mean Optical Power
Illuminated area	0.39	0.32	0.56	0.01
Duration		0.16	0.38	−0.16
Mean event radiance			0.73	0.16
Maximum event radiance				0.05

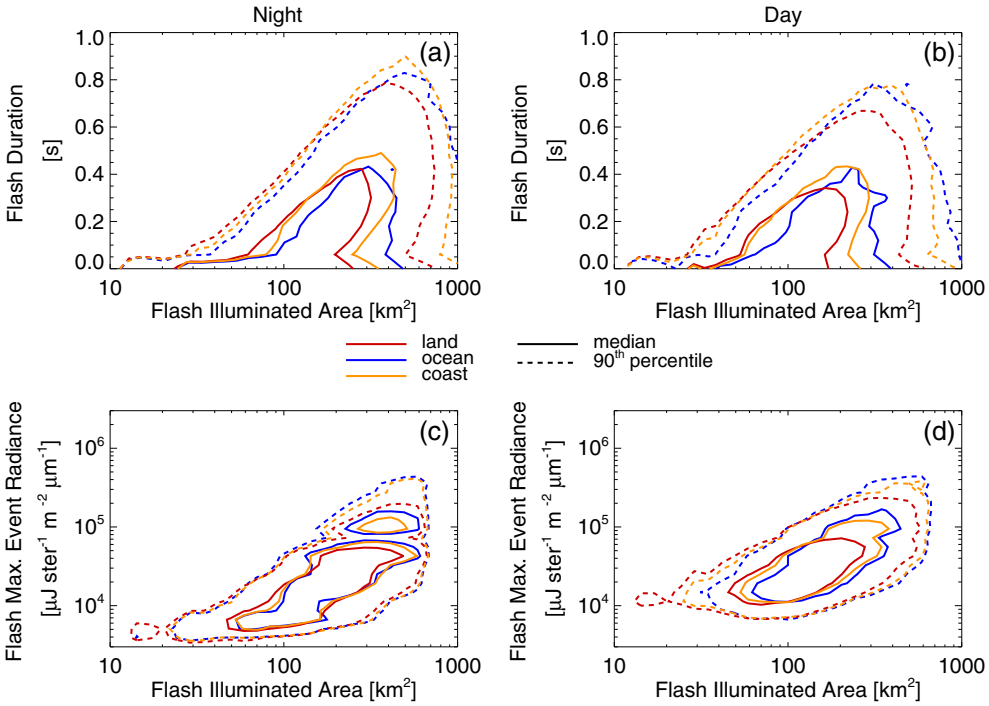

Figure 7. (a and b) Two-dimensional cumulative histograms of flash illuminated area and flash duration, (c and d) flash maximum event radiance, and (e and f) flash mean optical power for flashes in each sensitivity regime categorized by terrain type.

of their electrical structure, but, while bright flashes are often large and large flashes typically contain at least a few bright pixels, the range of possible maximum radiances for flashes of a given size can span an order of magnitude. For a given flash with an area of 200 km^2, for instance, the lower and upper intersects of the 90th percentile contours are around 10^4 and 10^5 μW m^{-2} ster^{-1} μm^{-1}, respectively.

3.3. Properties of the Cloud Environment at Lightning Flash Center Locations

[21] LIS observations are the result of a complex system that includes the optical properties of lightning flashes, the surrounding cloud medium, and even the LIS observing platform, itself. Scattering and attenuation of light from a lightning flash by the surrounding cloud can significantly affect its radiance observed from space. The importance of this effect is a considerable unknown, particularly since the LIS has no way of determining at what elevation lightning flashes occur. Two lightning flashes of the same size that give off the same amount of radiant energy may appear vastly different from above if one occurs below a thick layer of convective cloud while the other occurs at a higher altitude or embedded within the stratiform region.

[22] Effects of attenuation and scattering can be inferred from quartile distributions of flash coincident 85 GHz PCT for flashes grouped by mean optical power and maximum event radiance shown in Figure 8. In this figure, median, upper and lower quartile values of 85 GHz PCT are contoured for flashes of varying brightness. Flashes with particularly low mean optical powers tend to be associated with warmer PCTs than flashes with average overall brightnesses, resulting in a valley near 10^4 μW m^{-2} ster^{-1} μm^{-1} (Figures 8a and 8b). Particularly, dim coastal flashes, on the other hand, tend to be associated with much colder 85 GHz PCTs, even though the statistics of coastal flashes eventually merge with those for the other two terrain categories. Cold 85 GHz PCTs represent significant scattering by ice in the column near flash centers. Attenuation and scattering of optical radiance from flashes by large amounts of ice can make it more difficult to detect the flashes at lower altitudes or embedded within regions of strong convection. Because of this, dim flashes are observed more frequently in these regions. As flash mean optical power increases from typical values of around 10^4 μW m^{-2} ster^{-1} μm^{-1}, the median 85 GHz PCT increases from near 180 K to 220 K for all three terrain types at night and from 205 K to 240 K during the day. This statistical shift implies that particularly bright flashes tend to be located in weaker storm regions with relatively small amounts of ice.

[23] It is well known that oceanic convection is relatively weak compared to convection over land [e.g., *Zipser et al.*, 2006]. This would lead to oceanic environments and stratiform regions of convective systems being more favorable for particularly bright flashes from a radiance argument alone. Table 3 shows the fraction of stratiform flashes categorized by terrain type and flash illuminated area, mean optical power, and flash duration. While only 6% of all flashes coincide with stratiform rainfall, the largest and brightest flashes are much more likely to be stratiform flashes, regardless of terrain type. In contrast, the top 10% longest lasting flashes for each terrain type are either nearly equally as likely or even less likely to be stratiform than flashes overall.

[24] Still, while coincident 85 GHz PCTs tend to be lower for dimmer lightning flashes in terms of overall mean optical powers (Figures 8a and 8b), there is almost no relationship between environmental 85 GHz PCTs and maximum event

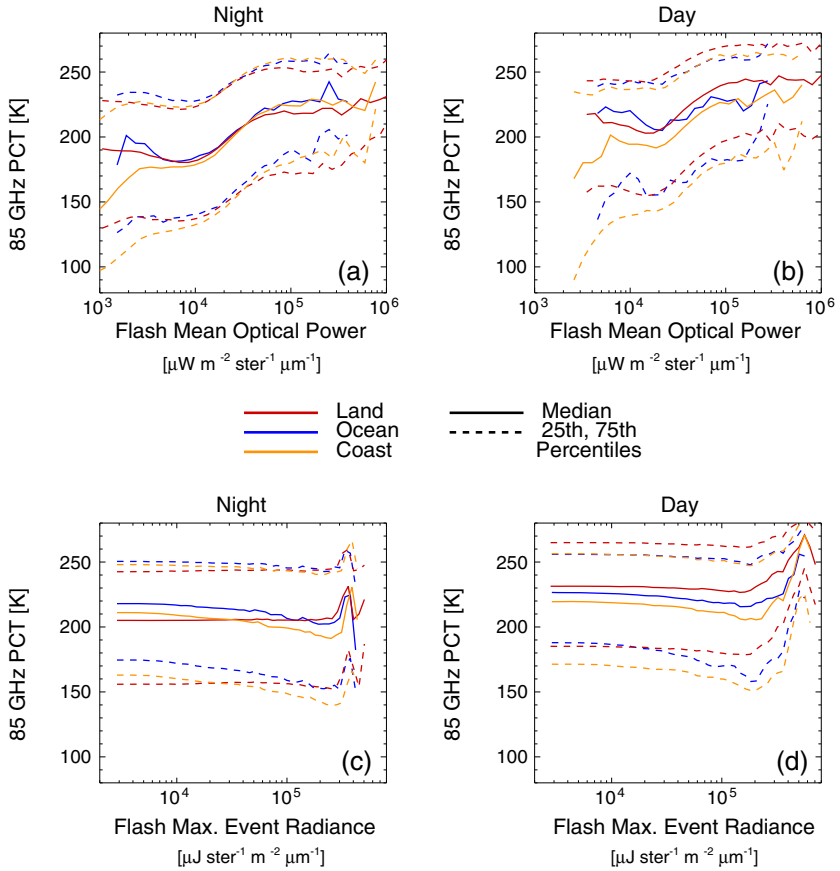

Figure 8. Flash coincident 85 GHz PCT quartile distributions by flash mean optical power for flashes at (a and c) night and (b and d) during the day categorized by terrain type. Distributions of 85 GHz PCT are created for bins of similar flash mean optical power and the quartiles of each bin are shown.

radiance (Figures 8c and 8d) below 10^5 μJ ster^{-1}m^{-2}μm^{-1}. The statistics are particularly consistent for dim flashes over land. Above this value, however, the brightest flashes in terms of peak radiance tend to occur in regions with warmer 85 GHz PCTs. Distributions of coincident 85 GHz PCTs with varying flash illuminated area are shown in Figures 9a and 9b. Exceptionally large flashes tend to be centered in regions with warm 85 GHz PCTs. Note that center location of flashes becomes more and more arbitrary with increasing flash size. At the same time, distributions of coincident 85 GHz PCTs for flashes of various durations in Figures 9c and 9d show that flashes lasting longer than 2/10 of a second are associated with colder 85 GHz PCTs and stronger convection than very short duration flashes. One possible reason for this is that these flashes most likely occur within the convective core, where lightning flashes are more frequent and the LIS algorithms may have a hard time separating unique flashes, allowing for multiple flashes to be combined and appear to last longer than each flash individually.

3.4. Properties of Parent Thunderstorms

[25] The state of the viewing medium certainly affects the perceived optical properties of lightning flashes; however, the overall convective properties of the storms, themselves,

Table 3. Fractions of All Flashes, Flashes With Near Median (45%–55%), and Flashes With Top 10% Values of Flash Illuminated Area, Duration, and Mean Optical Power for Each Terrain Type That Are Centered in Regions With Stratiform Precipitation Determined From Precipitation Radar Observations [*Awaka et al.*, 1998, 2009]

Stratiform Frequency	Terrain	All Flashes	Near Median	Top 10%
Categorized by flash area	land	5.5%	4.4%	11%
	ocean	10.2%	8.4%	13.3%
	coast	7%	5.9%	11.2%
Categorized by flash duration	land	5.5%	4.3%	9.6%
	ocean	10.2%	7.4%	15.4%
	coast	7%	5.2%	12.2%
Categorized by flash mean optical power	land	5.5%	4.3%	6.2%
	ocean	10.2%	8.4%	7.6%
	coast	7%	5.6%	5.8%

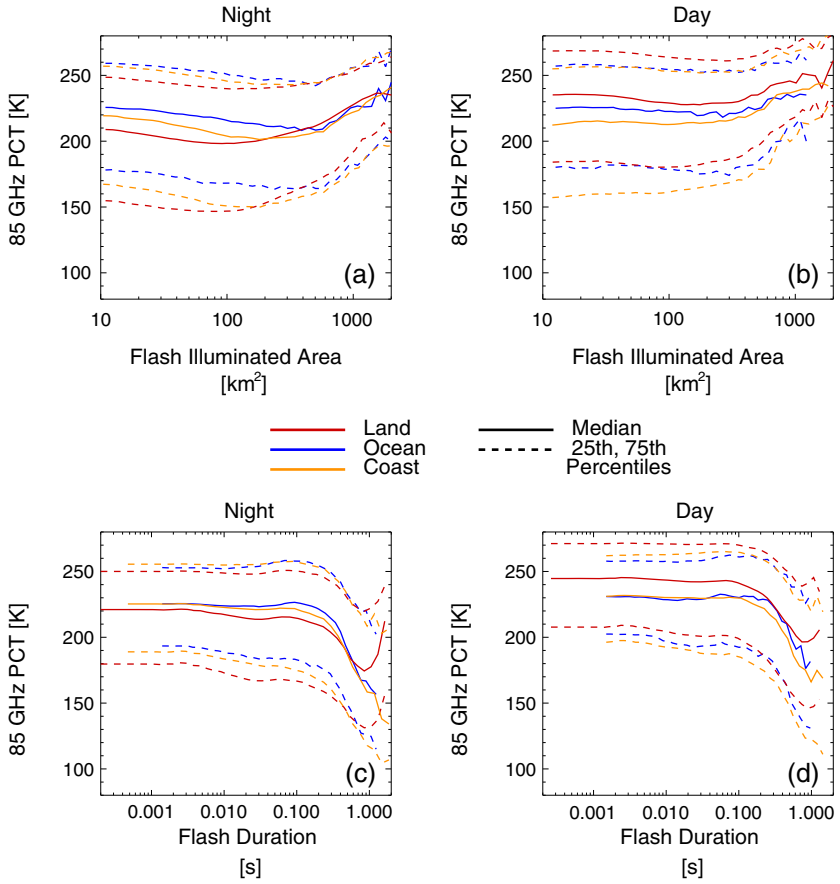

Figure 9. Flash coincident 85 GHz PCT quartile distributions by flash duration for flashes at (a and c) night and (b and d) during the day categorized by terrain type.

may also have an impact on the sizes, durations, and brightnesses of the lightning flashes that are observed. Radar Precipitation Features (RPFs) are used to examine how LIS-observed lightning flash characteristics relate to the properties of the parent storm system. RPFs are defined as contiguous regions of TRMM PR raining pixels, and the properties of these features are catalogued in the University of Utah precipitation feature database [*Liu et al.*, 2008]. For each feature with lightning, the maximum illuminated area, event radiance, and duration of all the flashes associated with the feature are summarized.

[26] Figure 10 shows the median values of associated RPF minimum 85 GHz PCTs categorized by RPF maximum flash area (Figure 10a), duration (Figure 10b), and brightness (Figure 10c). Exceptional flashes tend to be associated with RPFs that have colder minimum 85 GHz PCTs indicative of more ice and stronger convection, while those with only small, short lasting, and dim flashes are more likely to have

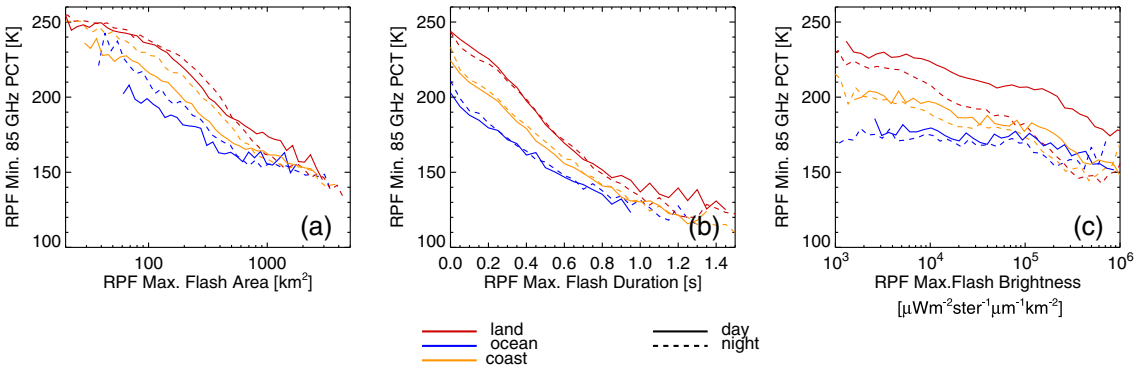

Figure 10. Median values of parent RPF minimum 85 GHz PCT categorized by (a) RPF maximum flash illuminated area, (b) RPF maximum flash duration, and (c) RPF maximum flash overall brightness in terms of mean optical power for flashes categorized by terrain type and sensitivity regime. The median curves are calculated using the same method as the quartile distributions in Figures 8 and 9.

Table 4. Median Properties of RPFs With Flashes Categorized by RPF Maximum Flash Illuminated Area, Duration, and Mean Optical Power[a]

		RPF Max. Flash Area		RPF Max. Flash Duration		RPF Max. Flash Mean Optical Power	
RPF mean:	Terrain	Median	Top 10%	Median	Top 10%	Median	Top 10%
Area (km^2)	land	2,236	7,918	2,089	8,216	2,114	6,459
	ocean	10,528	12,614	9,537	15,543	8,883	15,373
	coast	6,110	9,182	5,161	11,400	4,444	11,227
Flash count (#)	land	7.0	23.0	4.0	35.6	5.1	24.6
	ocean	3.6	9.8	2.3	16.7	3.0	10.3
	coast	5.6	17.5	2.9	28.6	4.5	19.3
20 dBZ Echo top (km)	land	11.4	13.3	11.2	13.6	11.5	12.4
	ocean	11.3	12.4	11.0	12.6	11.4	10.7
	coast	11.7	13.3	11.4	13.6	11.9	12
30 dBZ Echo top (km)	land	9.0	10.7	8.7	11.5	9.0	10.3
	ocean	8.6	9.7	8.2	10.5	8.7	8.5
	coast	8.9	10.4	8.4	11.4	9.0	9.6
Min. 85 GHz PCT (K)	land	199.6	162.7	208.5	146.8	202.3	177.4
	ocean	169.4	155.9	178.1	135.4	172.9	165.4
	coast	180.9	156.7	191.3	136.5	184.5	166.4
Min. 37 GHz PCT (K)	land	264.4	250.4	268.6	240.0	266.3	253.0
	ocean	255.9	250.8	259.5	239.2	257.8	250.1
	coast	259.8	250.5	264.6	238.4	262.2	250.0
Min. IR Tb (K)	land	213.4	200.0	215.2	199.9	214.0	208.4
	ocean	210.5	204.8	211.8	204.7	210.3	213.4
	coast	208.4	200.3	210.1	199.5	208.7	207.9
Volumetric rain (km^2 mm/h)	land	9,838	38,623	8,856	41,816	9,265	31,872
	ocean	50,834	63,974	44,797	82,817	41,706	77,386
	coast	29,089	48,239	24,202	61,750	21,210	58,180

[a]Near median (45th to 55th percentile) and top 10% RPF maximum flash properties are shown for land, ocean, and coastal flashes.

warmer minimum 85 GHz PCTs. Additional RPF properties categorized by mean and exceptional values of flash peak area, duration, and brightness are listed in Table 4. Compared to RPFs with only typical maximum flash properties, those with exceptional flashes not only have lower 85 GHz PCTs as seen in Figure 10, but they also tend to be larger in size, have higher flash counts, larger rain volumes, higher echo top heights, and colder 37 GHz PCTs.

[27] It may seem contradictory that even though exceptional flashes are often centered in storm regions with weak reflectivity and high microwave brightness temperatures, they are still more likely to occur in large systems with strong convection as opposed to small, isolated thunderstorms. However, differences in median RPF 85 GHz PCTs on the order of 100 K between RPFs with only small flashes and those with large flashes seem to indicate that storm structure plays a key role in determining the optical properties of these flashes. Because of this, the properties of lightning may be different for different stages of convection, though TRMM is unable to observe the life history of convection since it only provides snapshots of individual storms. To get around this, a statistical overview of diurnal cycles for each of the three categories of exceptional flashes and typical RPF properties throughout the day for land, ocean, and coastal regions is shown in Figure 11. The distributions of lightning and RPF properties have been diurnally normalized by scaling the values so that the diurnal maximum is 1 for easy comparison of relative phase. Though the diurnal cycles of large, bright, and long-lasting flashes are similar to that of all lightning, the timing of each peak is different. Over land, bright flashes reach their peak frequency early in the day compared to large and long-lasting flashes, with a maximum at around 3:00 PM local time. In contrast, long-lasting and

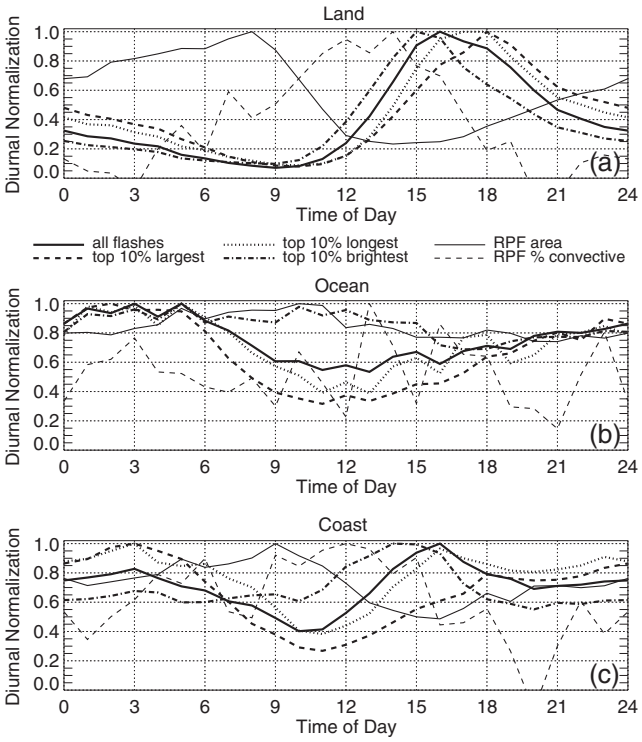

Figure 11. Normalized diurnal distributions of all flashes, and the top 10% largest, longest duration, and brightest flashes (a) over land, (b) oceanic, and (c) coastal regions. Diurnal normalized distributions of the properties of typical RPFs in each region are also shown, including mean RPF area and the fraction of convective precipitation indicated by 2A23 PR algorithm [*Awaka et al*., 1998, 2009].

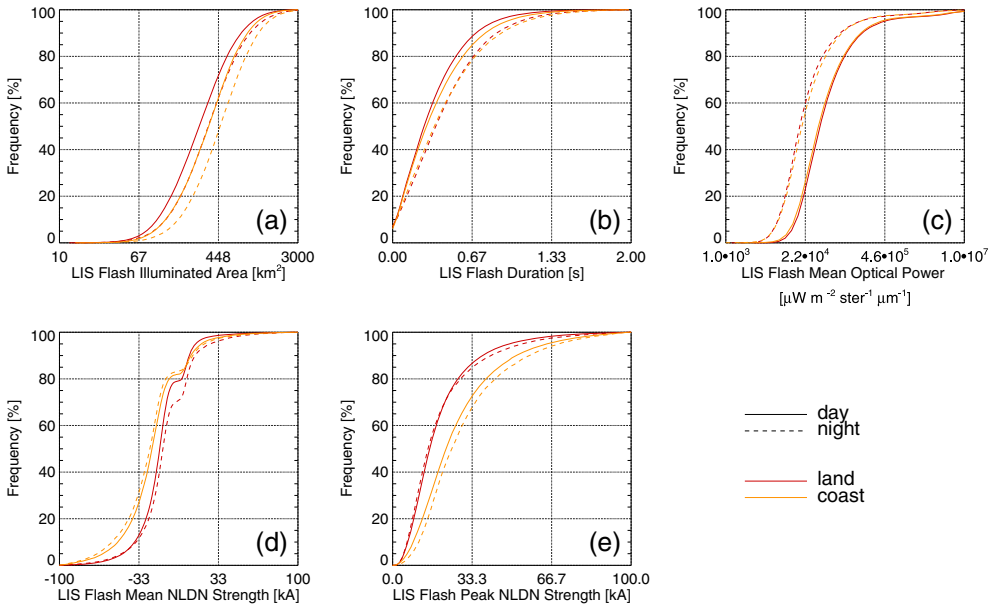

Figure 12. (a) CDFs of LIS flash illuminated area, (b) LIS flash duration, (c) LIS mean optical power, (d) mean NLDN-collocated strength, and (e) peak NLDN-collocated strength for flashes categorized by terrain type and LIS sensitivity regime.

large flashes are most common in the evening, between 5:00 and 6:00 PM local time.

[28] Afternoon thunderstorms over land around 3:00 PM tend to be rather small, and more convective in nature, as they tend to be in an earlier stage of convection and have not had much of a chance to develop into massive convective systems. There are likely smaller regions of thick cloud that can scatter and attenuate lightning flash radiance, allowing flashes to appear brighter. However, as the convection develops and organizes, convective cores are able to generate high flash rates, leading to flash overlap and a peak in long-lasting flashes around 5:00 PM. As the day wears on, thunderstorms reach their mature stage and develop significant regions of stratiform precipitation, which are more favorable for large flashes. Over the ocean, there is next to no phase difference between all flashes and the top 10% largest and longest lasting flashes, and the brightest flashes with the highest mean optical power are nearly equally common throughout the day. Thunderstorms over the open ocean are slightly larger in the late morning. Coastal regions (Figure 11c) have intermediate statistics between those for land and ocean, with a bimodal pattern including peaks in the early afternoon and early morning.

3.5. NLDN Properties of Collocated LIS Flashes Over the Southern United States

[29] In order to address the inability of the LIS to observe the electromagnetic element of lightning flashes, National Lightning Detection Network (NLDN) observations of lightning over the United States are examined alongside LIS data. Unlike TRMM, which makes a finite number of overpasses over the southern United States each day, allowing the LIS to view lightning in roughly 80 s increments, the NLDN is continuous and spans the entire country throughout the entirety of the LIS era [*Orville*, 2008]. The methodology employed in this study to assign NLDN flashes to LIS optical features is multifaceted. First, NLDN flashes that have greater horizontal uncertainty than typical LIS pixel sizes are removed. Next, the components (event pixels, groups, and flashes) of each LIS flash are analyzed to determine whether they have any NLDN counterparts. NLDN flashes that occur within 5 km of a LIS event pixel and that occur either within the timeframe between the first and last observed LIS group or 0.1 s from the mean observation time, whichever is larger, are considered. In cases where events from multiple LIS flashes attempt to claim a single NLDN flash, the NLDN flash is skipped entirely. Once NLDN strokes have been tied to a LIS event pixel, the LIS data hierarchy can then be used to find the flash and group associated with that pixel. In total, 208,805 NLDN flashes have been assigned to 205,151 unique LIS event pixels that form part of 203,142 independent groups and 190,031 unique LIS flashes observed between 1998 and 2011. These strict requirements for associating NLDN flashes to LIS features lead to flashes typically having only one valid NLDN collocation, even though flashes, groups, and even events with multiple NLDN associations are common. In the sample of collocated lightning flashes, negative polarity LIS flashes make up the majority of flashes (74.7%), while a smaller number of positive polarity LIS flashes (22.5%) and a miniscule of "mixed" polarity LIS flashes (2.8%) are present. All of these flashes are confined to land and coastal terrain categories, since the lack of sensors over the ocean leads to greater uncertainties.

[30] Figure 12 shows LIS and NLDN statistics of collocated flashes over land and coastal regions. As before with the global statistics (Figure 4), coastal flashes observed by LIS tend to be larger and longer lasting than flashes over land, while flash overall brightness does not deviate much between land and coast. Also, nighttime flashes are larger, last longer, and dimmer compared to daytime flashes. In addition to these LIS parameters, Figures 12d–12f show CDFs of the properties of NLDN strokes associated with these LIS flashes. Most NLDN strokes in this sample have negative polarity (Figure 12d), though coastal flashes are more likely to be

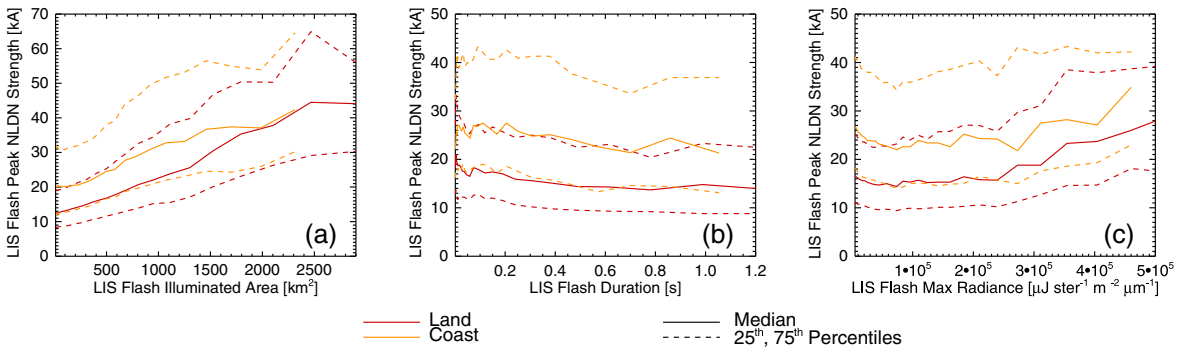

Figure 13. Collocated NLDN peak strength quartile distributions by (a) LIS flash illuminated area, (b) LIS flash duration, and (c) LIS flash maximum event radiance categorized by terrain type.

negative than flashes over land (81.4% as opposed to 74.3%). At the same time, the absolute value of NLDN flash strength is significantly greater in flashes over coastal regions (48.3% grater overall) than flashes over land. This can either be due to actual differences in the properties of lightning strikes over coastal regions, a lack of offshore sensors, or perhaps both.

[31] Figure 13 shows quartile distributions of NLDN strength for flashes grouped by collocated LIS flash illuminated area (Figure 13a), LIS flash duration (Figure 13b), and LIS flash maximum event radiance (Figure 13c). LIS flashes with larger areas and higher maximum radiances tend to have greater NLDN strengths, while longer duration LIS lightning flashes tend to have slightly weaker NLDN strengths. The statistics for NLDN strength and LIS flash area are separated for flashes of both positive and negative polarity in Figure 14, which shows the full probability distribution function (PDF) distribution for each bin (color contour) as well as 2-D histograms (line contour). Peak probabilities are also shown as thick lines for each branch. Even though most flashes are negative, resulting in the negative bias in Figure 13, this trend of large flashes being associated with stronger discharges holds true for positive flashes as well in both land and coastal regions, providing further evidence that the electrical and radiative properties of lightning flashes are interrelated.

4. Summary

[32] Statistics of lightning flash illuminated area, duration, peak event radiance, and mean optical power are examined globally from 12 years of TRMM LIS observations. Flashes over the open ocean are shown to be larger, to last longer, and to be optically brighter on average than those over land, which is consistent with past studies [*Boccippio et al.*, 2000; *Mach et al.*, 2011]. Moreover, coastal flashes are shown to have longer durations than those over land and over the ocean.

[33] Only weak correlations are found among flash illuminated area, duration, and maximum event radiance. Dim flashes occur more frequently over the regions with cold 85 GHz PCTs, implying that significant amounts of ice scattering affect flash-observed radiances. Exceptionally long-lasting flashes also occur more frequently in the regions with cold 85 GHz PCTs, and are possibly inseparable amalgamations of multiple flashes in intense convective regions with high flash rates. Flashes with large areas and long durations are more common in regions of stratiform precipitation.

[34] The diurnal distributions of exceptional flashes over land differ significantly in phase with one another and all lightning, overall. The top 10% brightest flashes are most common an hour earlier in the afternoon over land than all flashes, while the top 10% largest and longest lasting flashes

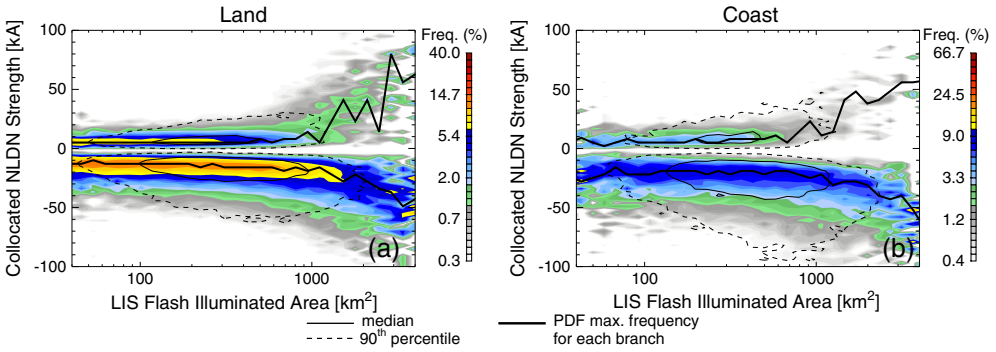

Figure 14. Histogram distributions (colored contour) of NLDN flash strength for flashes of various LIS illuminated areas for flashes over (a) land and over the (b) coastal ocean. The integrated sum of the contour for each LIS illuminated area bin is 100%. Two peak probability curves (thick lines)—one for positive polarity flashes and one for negative polarity flashes—as well as two-dimensional histograms of sample density (thin lines) are overlain.

peak 2 h later. At the same time, large, long-lasting, and bright flashes are more likely to occur in large thunderstorms with significant regions of strong convection, despite the fact that flashes with large illuminated areas and mean optical powers tend to occur in regions with relatively weak convective proxy values, including storm area, flash count, PR echo top heights, minimum TMI PCTs at both 85 GHz and 37 GHz, minimum IR temperature, and volumetric rain totals.

[35] Collocating NLDN data with LIS adds another perspective. The electromagnetic strength of lightning strikes detected by the NLDN is significantly greater over coastal regions than over land, though the lack of oceanic sensors may be responsible for at least some of this difference. Also, the largest and brightest flashes correspond to more powerful NLDN strokes. Because of this, it is possible that particularly large flashes are the result of powerful discharges from strong convective systems that propagate over relatively long distances rather than being simply regular flashes that occur in regions with minimal radiance attenuation that would cause them to appear larger.

[36] The above results indicate that the lightning properties over land and ocean are very different. Though relatively rare, stronger oceanic lightning flashes may contribute differently to the global electric circuit than lightning over land, as suggested in *Mach et al*. [2011]. Because of the considerable differences in the properties of thunderstorms between land and ocean, as well as the properties of individual lightning flashes, it is important to take land and ocean differences into account when ingesting the lightning observations into forecast and climate models.

[37] **Acknowledgments.** This research was supported by NASA Precipitation Measurement Mission grants NAG5-13628 and NNX11AG31G under the direction of Ramesh Kakar and NASA grant NNX08AK28G under the direction of Erich Stocker. Thanks also go to Erich Stocker and John Kwiatkowski and the rest of the Precipitation Processing System (PPS) team at NASA Goddard Space Flight Center, Greenbelt, MD, for data processing assistance.

References

Awaka, J., T. Iguchi, and K. Okamoto (1998), Rain type classification algorithm, *Meas. Precip. Space*, *3*, 213–224.

Awaka, J., T. Iguchi, and K. Okamoto (2009), TRMM PR standard algorithm 2A23 and its performance on bright band detection, *J. Meteorol. Soc. Jpn.*, *87a*, 31–52.

Betz, H. D., U. Schumann, and P. Laroche (2009), *Lightning: Principles, Instruments and Applications: Review of Modern Lightning Research*, 641 pp., Springer, Science, New York, NY.

Blakeslee, R. J., D. M. Mach, M. G. Bateman, and J. C. Bailey (2012), Seasonal variations in the lightning diurnal cycle and implications for the global electric circuit, *J. Atmos. Res.*, doi:10.1016/j.atmosres.2012.09.023.

Boccippio, D. J., W. Koshak, R. Blakeslee, K. Driscoll, D. Mach, D. Buechler, W. Boeck, H. J. Christian, and S. J. Goodman (2000), The Optical Transient Detector (OTD): Instrument characteristics and cross-sensor validation, *J. Atmos. Oceanic Technol.*, *17*, 441–458.

Boccippio, D. J., W. Koshak, and R. Blakeslee (2002), Performance assessment of the Optical Transient Detector and Lightning Imaging Sensor. Part I: Predicted diurnal variability, *J. Atmos. Oceanic Technol.*, *19*, 1318–1332.

Carey, L. D., M. J., Murphy, T. L. McCormick, and N. W. S. Demetriades (2005), Lightning location relative to storm structure in a leading-line, trailing-stratiform mesoscale convective system, *J. Geophys. Res.*, *110*, D03105, doi:10.1029/2003JD004371.

Cecil, D. J., S. J. Goodman, D. J. Boccippio, E. J. Zipser, and S. W. Nesbitt (2005), Three years of TRMM precipitation features. Part I: Radar, radiometric, and lightning characteristics, *Mon. Weather Rev.*, *133*, 543–565.

Christian, H. J., et al. (2003), Global frequency and distribution of lightning as observed from space by the Optical Transient Detector, *J. Geophys. Res.*, *108*(D1), 4005, doi:10.1029/2002JD002347.

Füllekrug, M., C. Price, Y. Yair, and E. R. Williams (2002), Intense oceanic lightning, *Ann. Geophys.*, *20*, 133–137.

Hendon, H., and K. Woodberry (1993), The diurnal cycle of tropical convection, *J. Geophys. Res.*, *98*, 16,623–16,637.

Kuhlman, K. M., D. R. MacGorman, M. I. Biggerstaff, and P. R. Kreibiel (2009), Lightning initiation in the anvils of two supercell storms, *Geophys. Res. Lett.*, *36*, L07802, doi:10.1029/2008GL036650.

Kummerow, C., W. Barnes, T. Kozu, J. Shiue, and J. Simpson (1998), The Tropical Rainfall Measuring Mission (TRMM) sensor package, *J. Atmos. Oceanic Technol.*, *15*, 809–817.

Lang, T. J., S. A. Rutledge, and K. C. Wiens (2004), Origins of positive cloud-to-ground lightning in the stratiform region of a mesoscale convective system, *Geophys. Res. Lett.*, *31*, L10105, doi:10.1029/2004GL019823.

Lay, E. H., A. R. Jacobson, R. H. Holzworth, C. J. Rodger, and R. L. Dowden (2007), Local time variation in land/ocean lightning flash density as measured by the World Wide Lightning Location Network, *J. Geophys. Res.*, *112*, D13111, doi:10.1029/2006JD007944.

Liu, C., and E. J. Zipser (2008), Diurnal cycles of precipitation, clouds, and lightning in the tropics from 9 years of TRMM observations, *Geophys. Res. Lett.*, *35*, L04819, doi:10.1029/2007GL032437.

Liu, C., E. J. Zipser, D. J. Cecil, S. W. Nesbitt, and S. Sherwood (2008), A cloud and precipitation feature database from 9 years of TRMM observations, *J. Appl. Meteor. Climate*, *47*, 2712–2728, doi:10.1175/2008JAMC1890.1.

Liu, C., D. Cecil, and E. J. Zipser (2011), Relationships between lightning flash rates and passive microwave brightness temperatures at 85 and 37 GHz over the tropics and subtropics, *J. Geophys. Res.*, *116*, D23108, doi:10.1029/2011JD016463.

Liu, C., D. J. Cecil, E. J. Zipser, K. Kronfeld, and R. Robertson (2012), Relationships between lightning flash rates and radar reflectivity vertical structures in thunderstorms over the tropics and subtropics, *J. Geophys. Res.*, *117*, D06212, doi:10.1029/2011JD017123.

Mach, D. M., H. J. Christian, R. J. Blackeslee, D. J. Boccippio, S. J. Goodman, and W. L. Boeck (2007), Performance assessment of the Optical Transient Detector and Lightning Imaging Sensor, *J. Geophys. Res.*, *112*, D09210, doi:10.1029/2006JD007787.

Mach, D. M., R. J. Blakeslee, M. G. Bateman, and J. C. Bailey (2010), Comparisons of total currents based on storm location, polarity, and flash rates derived from high-altitude aircraft overflights, *J. Geophys. Res.*, *115*, D03201, doi:10.1029/2009JD012240.

Mach, D. M., R. J. Blakeslee, and M. G. Bateman (2011), Global electric circuit implications of combined aircraft storm electric current measurements and satellite-based diurnal lightning statistics, *J. Geophys. Res.*, *116*, D05201, doi:10.1029/2010JD014462.

Marshall, T. C., and W. C. Rust (1993), Two types of vertical electrical structures in stratiform precipitation regions of mesoscale convective systems, *Bull. Am. Meteorol. Soc.*, *74*, 2159–2170.

Marshall, T. C., M. Stolzenburg, P. R. Krehbiel, N. R. Lund, and C. R. Maggio (2009), Electrical evolution during the decay stage of New Mexico thunderstorms, *J. Geophys. Res.*, *114*, D02209, doi:10.1029/2008JD010637.

Nesbitt, S. W., and E. J. Zipser (2003), The diurnal cycle of rainfall and convective intensity according to three years of TRMM measurements, *J. Clim.*, *16*, 1456–1475.

Orville, R. E. (2008), Development of the National Lightning Detection Network, *Bull. Am. Meteorol. Soc.*, *89*, 182–190.

Peterson, M. J., and C. Liu (2011), Global statistics of lightning in anvil and stratiform regions over the tropics and subtropics observed by TRMM, *J. Geophys. Res.*, *116*, D23201, doi:10.1029/2011JD015908.

Spencer, R. W., H. G. Goodman, and R. E. Hood (1989), Precipitation retrieval over land and ocean with the SSM/I: Identification and characteristics of the scattering signal, *J. Atmos. Oceanic Technol.*, *6*, 254–273.

Stolzenburg, M., T. C. Marshall, W. D. Rust, and B. F. Smull (1994), Horizontal distribution of electrical and meteorological conditions across the stratiform region of a mesoscale convective system, *Mon. Weather Rev.*, *122*, 1777–1797.

Toracinta, E. R., D. J. Cecil, E. J. Zipser, and S. W. Nesbitt (2002), Radar, passive microwave and lightning characteristics of precipitating systems in the tropics, *Mon. Weather Rev.*, *130*, 802–824.

Turman, B. N. (1977), Detection of lightning superbolts, *J. Geophys. Res.*, *82*, 2566–2568.

Williams, E. R. (2005), Lightning and climate: A review, *Atmos. Res.*, *76*, 272–287.

Williams, E. R., and G. Sátori (2004), Lightning, thermodynamic and hydrological comparison of the two tropical continental chimneys, *J. Atmos. Sol. Terr. Phys.*, *66*, 1213–1231.

Zipser, E. J., D. J. Cecil, C. Liu, S. W. Nesbitt, and D. P. Yorty (2006), Where are the most intense thunderstorms on Earth?, *Bull. Am. Meteorol. Soc.*, *87*, 1057–1071.